New Phytologist

Methods

Association between sap flow-derived and eddy covariance-derived measurements of forest canopy CO_2 uptake

Tamir Klein[1,2], Eyal Rotenberg[1], Fyodor Tatarinov[1] and Dan Yakir[1]

[1]Department of Earth and Planetary Sciences, Weizmann Institute of Science, Rehovot 76100, Israel; [2] Present address: Institute of Botany, University of Basel, Schoenbeinstrasse 6, Basel 4056, Switzerland

Author for correspondence:
Tamir Klein
Tel: +41 76 4886212
Email: tamir.klein@unibas.ch

Received: *22 May 2015*
Accepted: *8 July 2015*

New Phytologist (2016) **209:** 436–446
doi: 10.1111/nph.13597

Key words: $\delta^{13}C$, carbon assimilation, gross primary productivity (GPP), leaf gas-exchange, vapor pressure deficit, water-use efficiency (WUE).

Summary

- The carbon sink intensity of the biosphere depends on the balance between gross primary productivity (GPP) of forest canopies and ecosystem respiration. GPP, however, cannot be directly measured and estimates are not well constrained. A new approach relying on canopy transpiration flux measured as sap flow, and water-use efficiency inferred from carbon isotope analysis (GPP_{SF}) has been proposed, but not tested against eddy covariance-based estimates (GPP_{EC}).
- Here we take advantage of parallel measurements using the two approaches at a semi-arid pine forest site to compare the GPP_{SF} and GPP_{EC} estimates on diurnal to annual timescales.
- GPP_{SF} captured the seasonal dynamics of GPP_{EC} ($GPP_{SF} = 0.99 \times GPP_{EC}$, $r^2 = 0.78$, RMSE = 0.82, $n = 457$ d) with good agreement at the annual timescale (653 vs 670 g C m^{-2} yr^{-1}). Both methods showed that GPP ranged between 1 and 8 g C m^{-2} d^{-1}, and the GPP_{SF}/GPP_{EC} ratio was between 0.5 and 2.0 during 82% of the days. Carbon uptake dynamics at the individual tree scale conformed with leaf scale rates of net assimilation.
- GPP_{SF} can produce robust estimations of tree- and canopy-scale rates of CO_2 uptake, providing constraints and greatly extending current GPP_{EC} estimations.

Introduction

Forests play a major role in the terrestrial carbon cycle through CO_2 assimilation, respiration, and sequestration (Luyssaert *et al.*, 2007; Bonan, 2008; Canadell & Raupach, 2008; Reichstein *et al.*, 2013). Gross primary productivity (GPP) of forest canopies has hence become an important measure of the carbon uptake of forests. Considering the effects of the increase in atmospheric CO_2,on the one hand, and the influence of climate change, on the other, GPP is central to our understanding of the responses of ecosystem and biosphere to change (Ciais *et al.*, 2005; Asaf *et al.*, 2013; Reichstein *et al.*, 2013). Currently, GPP is routinely calculated using eddy covariance (EC) from the difference between measured net ecosystem CO_2 exchange (NEE) and inferred daytime ecosystem respiration (R_e) extrapolating night-time EC measurements of respiration based on empirical temperature response equations (Aubinet *et al.*, 2000; Baldocchi, 2003; Reichstein *et al.*, 2005). For the past two decades, the EC method has been providing essential GPP data from sites across all major biomes and climate types (Luyssaert *et al.*, 2007). However, the EC approach has several limitations and uncertainties. Its application is limited to relatively large, homogeneous and flat terrains, and it is critically dependent on empirical extrapolation of the night-time measurements with significant uncertainties (e.g., Van Gorsel *et al.*, 2009). The difficulties in using the EC methodology to obtain a balanced ecosystem energy budget has also indicated significant uncertainties in EC flux estimates, with estimated precision of *c.* ± 20% at best (Baldocchi *et al.*, 2001), and in the range of corrections for the basic wind speed and direction (e.g. Nakai & Shimoyama, 2012). Although EC flux measurements are widely used, such estimates cannot yet be used as the accurate reference points for GPP and, ultimately, the large range of global GPP estimates (*c.* 100 to *c.* 150 Pg C yr^{-1}; Beer *et al.*, 2010) indicates the critical need for more constraints on GPP estimates across all scales.

Indeed, alternative approaches are being continuously developed. For example, recent new developments include flux measurements of carbonyl sulfide (Asaf *et al.*, 2013) and remotely sensed solar-induced chlorophyll fluorescence (Parazoo *et al.*, 2014). Recent studies pointed out the potential utility of using independent estimates of water use efficiency, WUE, and transpiration, T, to estimate GPP from the relationship of $WUE = GPP/T$ (Hu *et al.*, 2010; Wang *et al.*, 2013), where GPP is nearly identical with canopy photosynthetic assimilation (see the Materials and Methods section) and T is obtained from sap flow (SF) time series. For simplicity, this approach is termed here 'SF-derived GPP'. In contrast with the EC-derived GPP, the CO_2 uptake estimated by the SF-derived GPP approach relates directly to the trees (Fig. 1). Therefore, it has the potential to

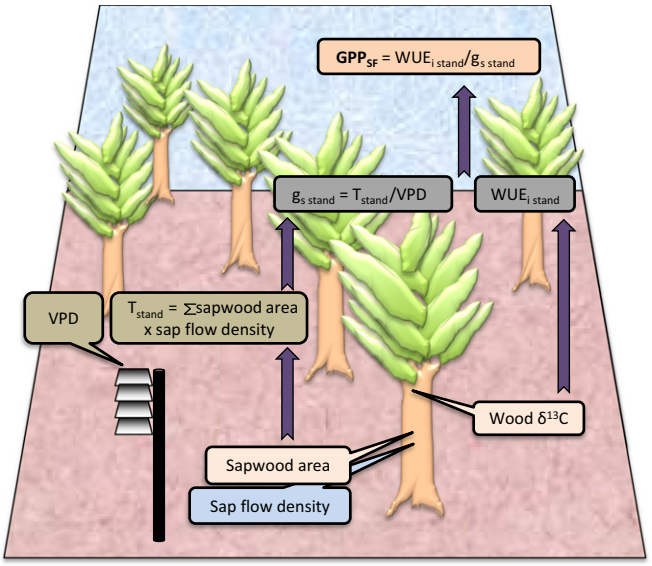

Fig. 1 Summary of measured and calculated variables (callouts and boxes, respectively) and equations used in the estimation of forest gross primary productivity (GPP) using the sap-flow method and the eddy covariance method (GPP_{SF} and GPP_{EC}, respectively). Tree measurements are described for one individual but need to be replicated in multiple trees. *T*, transpiration; VPD, vapor pressure deficit; g_s, stomatal conductance; WUE_i, intrinsic water-use efficiency. The background image shows a *Pinus halepensis* plot in Yatir forest.

partition the CO_2 uptake between overstory and understory and among co-occurring tree species.

Photosynthetic CO_2 assimilation (*A*) occurs via plant stomata in parallel with transpiration. At the leaf level, CO_2 uptake by photosynthesis is readily measured, along with leaf transpiration and stomatal conductance (g_s), using a chamber equipped with an infrared gas analyzer (Von Caemmerer & Farquhar, 1981). However, a chamber technique cannot be easily applied to mature forest trees, and is difficult to scale up to tree and canopy scales. Alternatively, transpiration (*T*) from a forest canopy can be more easily estimated by upscaling of SF measurements in individual trees (Granier, 1985; Cermak *et al.*, 2004; Tatarinov *et al.*, 2005; Cohen *et al.*, 2008). The ratio *A*/*T*, defined as water-use efficiency (WUE) is calculated at the leaf scale using simultaneous chamber measurements of *A* and *T*. Alternatively, an integrated value of intrinsic water use efficiency (WUE_i, the ratio A/g_s) can be calculated from the carbon isotope ratio ($\delta^{13}C$) in the assimilated carbon (Farquhar & Richards, 1984). The isotopic approach takes advantage of the inherent relationships between plant CO_2 discrimination and leaf internal CO_2 concentration, and the constant ratio of the diffusivities of CO_2 and water in air (Farquhar & Richards, 1984; Seibt *et al.*, 2008; Maseyk *et al.*, 2011). A tree-scale CO_2 uptake can be estimated if concurrent estimates of *T* and WUE values are obtained ($A_{tree} = T_{tree} \times WUE$). In extrapolating from leaf to canopy scales, *A* and GPP are often used interchangeably, in spite of a small difference (*c.* 10%; see the Materials and Methods section). Recently, the applicability of such an SF-based approach has been demonstrated in subalpine forest and subtropical plantation (Hu *et al.*, 2010; Wang *et al.*, 2013). SF methodology can overcome several of the EC limitations, providing a lower cost option that can be applied irrespective of topography and atmospheric fetch requirements, and rely on a smaller number of assumptions and corrections. Although these studies have been instrumental in introducing the concept, there is still an urgent need to test the SF-derived CO_2 uptake estimates against GPP calculated from EC measurements.

Here we compare a long-term EC-derived GPP (GPP_{EC}) at a 13-yr old fluxnet site at a semi-arid pine forest in Yatir, Israel, with SF-derived GPP (GPP_{SF}) from ten trees in two periods: 2005 and 2009–2010. These observation years capture contrasting periods in the history of this forest, providing some robustness to our analysis: Although 2005 was a peak growth year, 2009–2010 followed two consecutive drought years, resulting in *c.* 5% mortality (Klein *et al.*, 2014). Although significant uncertainties are still associated with the GPP_{EC}, as noted above, estimates for our specific forest site have been constrained by a range of independent measurements: latent heat flux measurements with fully closed energy balance indicated high reliability of the EC measurements at the site (Rotenberg & Yakir, 2010); estimating changes in biomass based on aerial photography (Bar Massada *et al.*, 2006); biomass inventories and long-term sum of respiration fluxes (Grünzweig *et al.*, 2003, 2007); and carbon sink estimates at the tree scale (Klein & Hoch, 2015). For example, an annual GPP_{EC} of 670 g C m^{-2} yr^{-1}, which is translated into 22.3 kg C per tree yr^{-1}, consistent (± 5%) with the sum of tree C sinks of 23.5 kg C per tree yr^{-1} (Klein & Hoch, 2015). Our study site offered parallel, long-term, continuous measurements of EC and SF, with minimum contribution of the understory vegetation and groundwater to the forest fluxes, and detailed *T* estimates, verified by a balanced water budget (*T* = precipitation – (evaporation + interception); Raz-Yaseef *et al.*, 2010; Klein *et al.*, 2014). Our objective was to exploit SF time series, combined with ^{13}C data, to estimate photosynthetic CO_2 uptake at the tree level and, consequently, GPP at the canopy scale, in comparison to the traditional GPP_{EC}.

Materials and Methods

Site description

Our study was conducted in Yatir forest, a 45-yr-old Aleppo pine (*Pinus halepensis* Miller) plantation located at the northern edge of the Negev desert, Israel (31°20′N, 35°20′E). The climate is hot and dry (40-yr average mean annual temperature and precipitation are 18.2°C and 285 mm). Stand density is *c.* 300 trees ha^{-1}, mean tree height is 10.2 ± 2.49 m and mean diameter at breast height (DBH) is 19.8 ± 5.61 cm. In 2000, an instrumented flux tower was erected in the geographic center of the forest, allowing continuous measurements of NEE and GPP (Grünzweig *et al.*, 2003; Rotenberg & Yakir, 2010). Unless specified, all measurements and samples were taken within the flux tower footprint. The study site offered an ideal setting to compare the two GPP estimation methods, because: (1) EC and SF were measured continuously during most of the period under study; (2) Canopy CO_2 uptake at the study site is almost entirely attributed to the trees' photosynthesis, with only minor contribution of understory vegetation (Grünzweig *et al.*, 2007); (3)

Changes in needle and wood $\delta^{13}C$ that were used for deriving the WUE_i were based on a 7-yr dataset (1997–2003) and therefore provided a robust representation of the seasonal changes in WUE_i; and (4) A phenological decoupling between stem wood growth in the wet season and needle formation in the dry season (Klein *et al.*, 2005; Maseyk *et al.*, 2008) ensured year-round availability of fresh plant material with carbon isotopic signals for WUE_i calculation.

Sap flow-derived canopy-scale assimilation rates

We developed an approach to estimate GPP in which we use the well-established physiological relationship: $WUE_i = A/g_s$ ($\mu mol\ CO_2\ mol^{-1}\ H_2O$). We wish to scale up to the ecosystem scale and solve for A_{stand}, assuming that at this scale $A_{stand} = GPP$. Leaf mitochondrial respiration, R_d, in the light is subtracted from the leaf-scale assimilation measurements (A). R_d is added back in estimating canopy GPP, with significant uncertainty (e.g. Speckman *et al.*, 2014), and neglecting downregulation of R_d in the daytime (e.g. Heskel *et al.*, 2014) when canopy-scale GPP is estimated based on extrapolating night-time ecosystem respiration, R_e (see more detail in Asaf *et al.*, 2013). Thus, GPP_{SF} was calculated from:

$$GPP_{SF} = WUE_{i\,stand}/g_{s\,stand}, \quad \text{Eqn 1}$$

which can be solved by obtaining independent estimates of WUE_i and g_s (Fig. 1; see Table 1 for list of variables used in this study). Here we estimate WUE_i from $\delta^{13}C$ measurements of organic material averaged for the stand (based on 11 *P. halepensis* trees growing on two plots in Yatir forest; see Supporting Information Methods S1), using the following equation (adapted from Farquhar & Richards, 1984; Seibt *et al.*, 2008):

$$WUE_i = C_a/r \times \{[b - \Delta - pr \times (\Gamma^*/C_a)]/[b - a + (b - a_m) \times (g_s/(r \times g_i))]\} \quad \text{Eqn 2}$$

Table 1 List of main variables used in this study

Symbol	Description	Units	Value range
A_{leaf}	Needle CO_2 assimilation	$\mu mol\ CO_2\ m^{-2}\ s^{-1}$	0.2–12.7
A_{tree}	Tree CO_2 assimilation	g C per tree d^{-1}	2.3–410.2
GPP	Gross primary productivity	g C $m^{-2}\ d^{-1}$	0.1–9.1
g_s	Stomatal conductance	mol $H_2O\ m^{-2}\ s^{-1}$	N/A
NEE	Net ecosystem CO_2 exchange	g C $m^{-2}\ d^{-1}$	N/A
R_e	Ecosystem respiration	g C $m^{-2}\ d^{-1}$	N/A
SF	Sap flow	kg $H_2O\ d^{-1}$	0.2–127.1
SFD	Sap flow density	$cm^3\ H_2O\ d^{-1}\ cm^{-2}$	6.4–291.6
SWA	Sapwood area	$cm^2\ ha^{-1}$	66 377–66 599
T_{stand}	Stand-level transpiration	$cm^3\ H_2O\ m^{-2}\ d^{-1}$	N/A
VPD	Vapor pressure deficit	kPa	0.0–6.9
WUE_i	Intrinsic water-use efficiency	$\mu mol\ CO_2\ mol^{-1}\ H_2O$	75.0–120.0

N/A, not available.

(C_a, atmospheric CO_2 concentration in ppm (continuously measured on site); r, ratio of the diffusivities of CO_2 and water vapor in air (1.6); a, a_m, b and pr, leaf-level discriminations against ^{13}C in the diffusion through the stomata (4.4‰), during dissolution and liquid phase diffusion (1.8‰), in biochemical CO_2 fixation (29‰), and in photo-respiratory CO_2 release (8‰), respectively; Δ, tree discrimination against ^{13}C; Γ^*, temperature-dependent CO_2 compensation point of *c.* 30–45 ppm (Maseyk *et al.*, 2008); g_s/g_i, ratio between stomatal and internal conductances to CO_2 respectively (0.5 according to Maseyk *et al.*, 2011)).

In order to obtain an estimate of $g_{s\,stand}$, we used measured tree transpiration and continuously monitored vapor pressure deficit (VPD) and the general relationship (Beer *et al.*, 2009):

$$g_s = T/VPD \quad \text{Eqn 3}$$

T was measured as sap flow (SF) of individual tress integrated over the daily cycle (to overcome 1–6 h offset between SF and T in the dry season). Notably, SF and $\delta^{13}C$-derived WUE_i (Eqn 2) integrate different spatial and temporal micro-meteorological changes across the canopy such as variations in light levels and aerodynamic conditions. SF sensors were installed on 16 trees in Yatir forest, 10–70 m from the flux tower in 2004 and again in 2009. Trees were chosen to capture the distribution of DBH and height of trees growing at the footprint of the flux tower. For our analysis, 10 out of 16 trees with the longest SF time-series were chosen. Lab-manufactured thermal dissipation sensors (Granier, 1985) were applied to all trees, and commercial heat balance sensors (Cermak *et al.*, 2004; EMS, Brno, Czech Republic) were also used on six of these trees. The correlation between the two methods had $r^2 = 0.90$, with heat balance sensors producing values 2.5 times higher than thermal dissipation sensors. The ratio of 2.5 was in agreement with the forest-scale water flux partitioning to tree transpiration calculated for the site (Klein *et al.*, 2014) and, independently, with earlier validations of the thermal dissipation method (Kanety, 2010; Steppe *et al.*, 2010; Paudel *et al.*, 2013) and was therefore used as a calibration factor. Radial and sapwood depth gradients of SF were measured and analyzed in these trees in a former study (Cohen *et al.*, 2008) and were used for the length compensation factor below. Measurements were taken every 30 s and the 30-min average was saved on a local CR1000 data-logger (Campbell Scientific Inc., Logan, UT, USA). Sap flux densities on the diurnal scale (SFD, in $cm^3\ d^{-1}\ cm^{-2}$) were calculated from thermal dissipation sensors in relation to the minimum sap flux during the day:

$$SFD = LCF \times CF \times \sum_{day} 0.04284 \times [(\Delta T_{max} - \Delta T_r)/\Delta T_r]^{1.231} \quad \text{Eqn 4}$$

(0.04284 ($kg\ m^{-2}\ s^{-1}$) and 1.231 are empirical constants (Granier, 1985); LCF = 1/0.65, the length compensation factor due to the inability of the 2-cm probes to capture the entire active sapwood depth, but rather 65% of it (for *P. halepensis* in Yatir; Cohen *et al.*, 2008; Paudel *et al.*, 2013) and calculated specifically for individual trees; CF, a calibration factor of 2.5; ΔT_r, average

half hourly temperature difference between heated and non-heated probes; ΔT_{max}, maximum temperature difference measured during the day (assumed to be at a negligible sap flow rate, below sensor sensitivity threshold) as in the empiric equation (Granier, 1985)). Radial SF gradients were observed in these trees, but were inconsistent with specific azimuths and smaller than differences between similar-size individuals (Cohen *et al.*, 2008). SFD was then scaled to the stand scale, after adjusting to total sapwood area per hectare, ΣSWA, based on the DBH distribution in forest inventory surveys conducted in 2005 and 2010 in the plots around the flux tower:

$$\sum \mathrm{SWA} = \sum_{i=5}^{35} (f_i \times \mathrm{SWA_i}) \qquad \text{Eqn 5}$$

(f_i, number of trees per hectare in DBH class i, between 5 and 35 cm, in 1 cm increments; $\mathrm{SWA_i}$, sapwood area of a tree at a certain DBH class in cm^2, considering a measured sapwood depth of 6 cm below the cambium (Cohen *et al.*, 2008)). Based on Eqn 4, the 2005 and 2010 ΣSWA were 66 377 and 67 599 $cm^2\ ha^{-1}$, respectively. These rather similar values were the result of a tradeoff between drought-induced growth reductions and tree mortality, on the one hand, and some diameter increment, on the other. T_{stand} was thus obtained:

$$T_{stand} = \sum \mathrm{SWA} \times \mathrm{SFD_{mean}} \qquad \text{Eqn 6}$$

In order to solve for $g_{s\ stand}$, diurnal T_{stand} values were divided by VPD, which was continuously monitored at the flux tower and averaged for each day with the following criteria, based on a previous study in the study site (Maseyk *et al.*, 2008): (1) Because CO_2 uptake is restricted to daytime hours, night-time VPD values were disregarded; (2) Because stomatal closure restricts CO_2 uptake to VPD < 4.0 kPa in *P. halepensis* in Yatir, the value of 4.0 kPa was used when measured VPD was above 4.0 kPa; and (3) Because CO_2 uptake is unaffected by VPD at VPD < 1.5 kPa in *P. halepensis* in Yatir, the value of 1.5 kPa was used when measured VPD was below 1.5 kPa. Using these criteria, the diurnal mean VPD avoided the bias associated with averaging low and high values that had negligible effect on CO_2 uptake. Similar procedures were also applied in earlier studies (Ewers & Oren, 2000; Drake *et al.*, 2011). The extent to which the continuously measured air VPD represented the actual VPD across the canopy and at the needle surface was further tested (Methods S2).

Tree-scale carbon assimilation and canopy-scale monthly and annual GPP

Tree-scale carbon assimilation rate (A_{tree}) was calculated similarly on diurnal timescale from the ratio $\mathrm{WUE_{i\ stand}}/g_s$. To test the seasonal dynamics of A_{tree}, leaf photosynthesis (A_{leaf}) was measured using the LiCor 6400 on the sample trees in the morning (09:00–11:00 h) and afternoon (12:00–14:00 h) during eight field days between 22 October 2009 and 8 December 2010. Both A_{tree} and the SF-derived GPP estimates were based on SF data availability, that is for 235 d in the calendar year 2005, and for the entire period between 1 October 2009 and 31 December 2010. Diurnal $\mathrm{GPP_{SF}}$ estimates were summed into an annual estimate for the hydrological year of 2010 (October 2009–October 2010) but not for 2005 due to large data gaps. Monthly $\mathrm{GPP_{SF}}$ values were calculated for all months except for March–June 2005 due to large data gaps. In other months of 2005, data gaps of 1–3 d were filled by the mean $\mathrm{GPP_{SF}}$ of the day before and the day after the gap. Two larger gaps of 12 and 11 d in July and September 2005, respectively, were filled by monthly mean values. In spite of the large gaps this approach was still safe considering the negligible $\mathrm{GPP_{SF}}$ variance in those months (1.0 ± 0.06 and 0.8 ± 0.05 g C $m^{-2}\ d^{-1}$, respectively).

Eddy covariance-derived GPP

Eddy covariance-derived GPP ($\mathrm{GPP_{EC}}$) was calculated from:

$$\mathrm{GPP_{EC}} = \mathrm{NEE} - R_e \qquad \text{Eqn 7}$$

(NEE, net ecosystem CO_2 exchange; R_e, ecosystem respiration). The NEE was measured continuously at the Yatir flux tower (Rotenberg & Yakir, 2010). Data gap filling and carbon flux partitioning were performed using an algorithm specially developed for the study site (Afik, 2009). Night-time NEE values with the friction velocity $U^* < U^*_{critical}$ were excluded. $U^*_{critical}$ was defined for each month as the value where the night-time NEE (U^*) dependence reached a plateau. Missing NEE values (including NEE night-time values when $U^* < U^*_{critical}$) were replaced by averages of NEE values for the day before and the day after the current day and for the same hour and minutes as the missing value (+½ h only if it was still in the same day). If the corresponding values in the closest days were also missing, longer series of close days were checked. The largest gaps that remained after the previous step were filled by the overall mean for a given hour taken within 30 d in the wet season (November to April) and within 60 d in the dry season. Specifically, night-time ecosystem respiration, R_{ne}, used for estimating R_e was calculated for each day as mean of the first 3 × 30-min periods of each night. In these periods, turbulent conditions are typically the highest during the night (Van Gorsel *et al.*, 2009) and better represent the previous daytime photosynthetic activities. Daytime respiration, R_{dt}, for each 30-min period was then calculated as:

$$R_{dt} = R_{ne} \times (\alpha_1 q_s^{\mathrm{d}T_s} + \alpha_2 q_w^{\mathrm{d}T_a} + \alpha_3 q_f^{\mathrm{d}T_a}) \qquad \text{Eqn 8}$$

(coefficients q_s, q_w, and q_f correspond to soil, wood and foliage Q10 values; $\mathrm{d}T_s$ and $\mathrm{d}T_a$, differences of temperatures between the target time of R estimate, and that at the beginning of the night for soil and air temperatures, respectively; partitioning coefficients α_1, α_2 and α_3 are 0.5, 0.1 and 0.4, respectively, representing the relative contribution to ecosystem CO_2 exchange of soil, wood, and foliage). q_s, q_w, and q_f were calculated based on Grünzweig *et al.* (2009): $q_s = 2.45$ for wet soil (soil water content in upper 30 cm above 20% v/v) and $q_s = 1.18$ for dry soil; $q_f = 3.15–0.036\ T_a$; and

$q_w = 1.34 + 0.46 \cdot \exp\left(-0.5 \cdot ((\text{DoY} - 162)/66.1)^2\right)$ (DoY, day of year). Needle respiration was measured directly using a gas exchange chamber over 24-h periods on seasonal and annual timescales, also accounting for needle phenology (Maseyk *et al.*, 2008). Profile CO_2 measurements showed that CO_2 storage in Yatir forest is rather small and can be ignored. Being an evergreen forest ecosystem at the dry timberline, interannual leaf area index variations are low and the contribution of understory vegetation is insignificant (Grünzweig *et al.*, 2003). This approach (Afik, 2009) was found to provide for our specific semi-arid site better results than the more conventional approach (Reichstein *et al.*, 2005) based on comparing predicted and measured soil respiration over the daily and seasonal cycles.

Statistical analysis

The significance of seasonal and interannual variations in δ^{13}C-derived WUE_i were tested in ANOVA using JMP Pro 11 (Cary, NC, USA) with WUE_i as response and month, or year (nested by month) as model effects, respectively. Variations in the estimation of GPP from Eqn 1 were calculated using the variations in its components (SFD, WUE_i and VPD) and applying error propagation rules (Taylor, 1997). If x and y have independent errors δx and δy, then the error in $z = x + y$ is $\delta z = (\delta x^2 + \delta y^2)^{1/2}$, and the error in $z = x \times y$ is $\delta z/z = ((\delta x/x)^2 + (\delta y/y)^2)^{1/2}$. In this analysis, we used standard errors of each component. Errors in the daily mean SFD were those associated with variations among the ten individual trees; errors in the monthly mean WUE_i were from interannual variations in 2001–2003; and errors in the daily mean VPD were from fluctuations in the half-hourly VPD values during daytime. The relationships between GPP_{SF} and GPP_{EC} were studied in ANOVA using JMP Pro 11. The interdiurnal co-variability between GPP_{SF} and GPP_{EC} and the relationships between the ratio GPP_{SF}/GPP_{EC} and environmental variables were studied using Statistica (StatSoft Inc., Tulsa, OK, USA).

Results

The seasonal SF dynamics of *Pinus halepensis* in Yatir forest have been described, and specifically for 2010 (Klein *et al.*, 2014). The SF rate correlated well with tree size (Fig. S1; $r^2 = 0.97$ in 1 May 2010 and $r^2 \approx 0.95$ and 0.70 during the wet and the dry seasons, respectively). As expected, when expressed on a sapwood area basis, that is, as sap flux density (SFD), the variation among trees decreased considerably, although it still existed (Fig. S1). Changes in *P. halepensis* δ^{13}C-derived WUE_i followed a seasonal pattern with minimum of 81.7 μmol CO_2 mol^{-1} H_2O in December, and maximum of 101.5 μmol CO_2 mol^{-1} H_2O in April (Fig. S2). The seasonal dynamics of δ^{13}C-derived WUE_i was significant ($P = 0.008$) but the interannual variation was not significant ($P = 0.574$). The δ^{13}C-derived WUE_i pattern was similar to that of the WUE_i calculated from chamber gas exchange measurements, but was more stable and had mostly lower values (Fig. S2). This was expected considering that gas exchange measurements were performed under saturating light conditions, thereby promoting higher A and WUE_i than under ambient conditions; and that the organic matter integrated the isotopic signals of CO_2 throughout the day and the month, which in the dry season (May–October) was assimilated under very low flux conditions.

In a tree with DBH of 22 cm during 2010, A_{tree} rates were 10–50 g C d^{-1} during the dry season (June–November; Fig. 2a). A_{tree} increased to 220 g C d^{-1} during the first major rain events marking the onset of the wet season in January, and up to 410 g C d^{-1} by the end of March. By the end of April, A_{tree} did not exceed 150 g C d^{-1} again, and decreased to dry season rates during May. In comparison, needle photosynthesis (A_{leaf}) measured in eight field days in 2010 showed a similar pattern (Fig. 2a). Both estimated A_{tree} and measured A_{leaf} had minimum rates during the dry season, with five-fold increase in rates in May, and 12-fold increase during March–April. The seasonal dynamics of tree transpiration (Fig. 2b) were generally similar to those of tree carbon uptake. The ratio A_{tree}/T_{tree} fluctuated between 1.9 mmol CO_2 mol^{-1} H_2O in early September–October and 5.7 mmol CO_2 mol^{-1} H_2O in April–May (Fig. 2b). A_{tree}/T_{tree} had many short-term oscillations reflecting the high variability of VPD. Overall, the range in A_{tree}/T_{tree} was three-fold, whereas T_{tree} changes were 12-fold or higher. This meant that the T_{tree} and A_{tree} curves were generally well correlated.

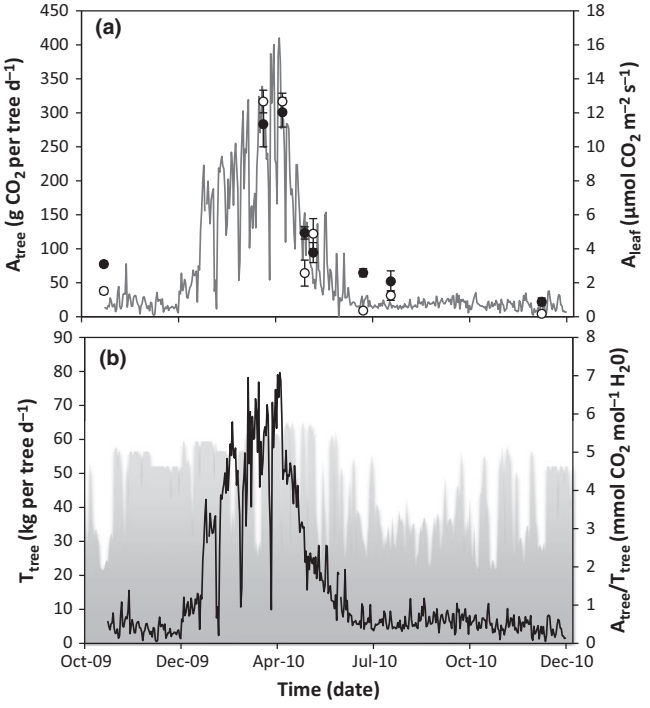

Fig. 2 Tree-scale (22 cm diameter at breast height (DBH) *Pinus halepensis* tree at the observation plot in Yatir forest in 2010) CO_2 uptake (A_{tree}; a), transpiration (T_{tree}; b), and WUE_{tree} (A_{tree}/T_{tree}; gray area in b), derived from sap-flow measurements, and leaf-scale rates of CO_2 uptake (A_{teaf}; a) obtained from eight field measurements days between 22 October 2009 and 8 December 2010 on needles of the same tree (or trees of similar age and size, and at the same stand density) in the morning (closed circles) and afternoon (open circles). Error bars represent standard errors of the mean ($n = 3$–6).

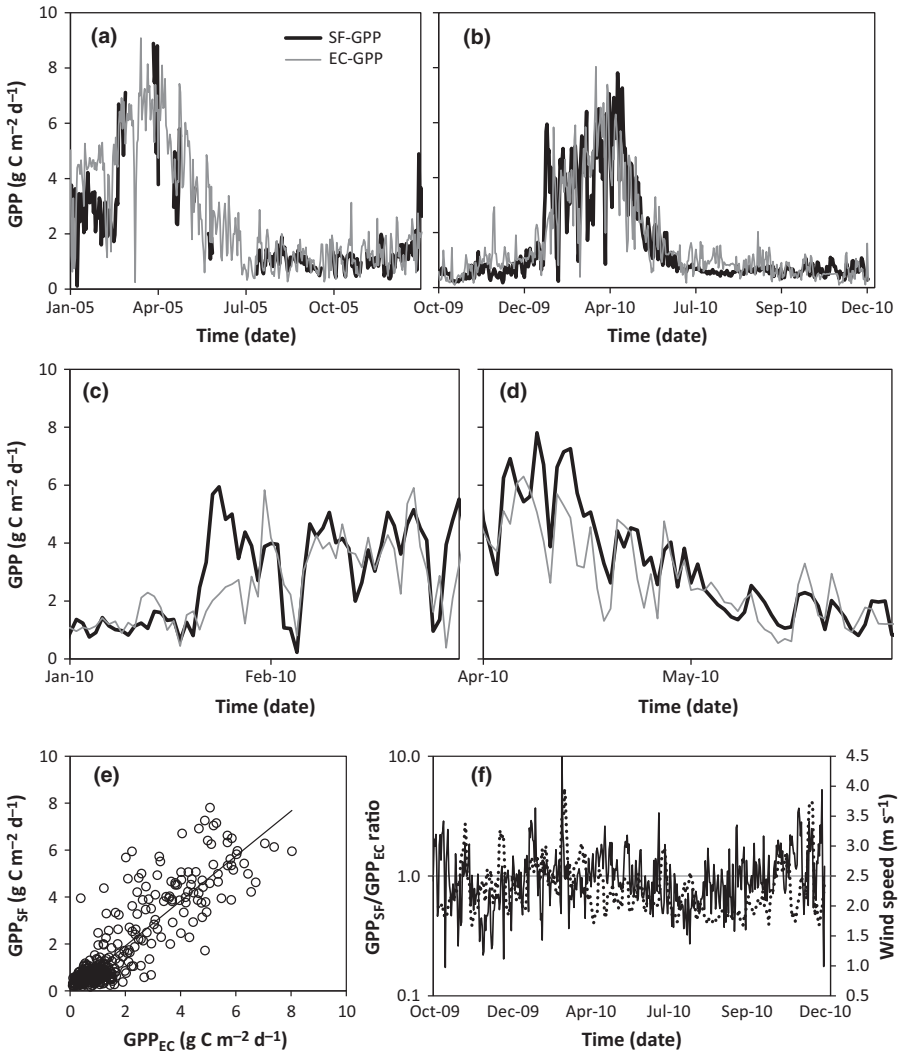

Fig. 3 Comparison between sap flow-derived and eddy covariance-derived gross primary productivity (GPP) in Yatir forest in 2005 (a) and 2010 (b), with close-up on January–February 2010 (c) and April–May 2010 (d). Correlation between daily values of sap flow-derived and eddy covariance-derived GPP in 2009–2010 (e) yielded the linear fit: ($GPP_{SF} = 0.987 \times GPP_{EC}$), $r^2 = 0.78$, $P < 0.0001$, $n = 457$ d. GPP_{SF}/GPP_{EC} ratio (logarithmic scale; black line) and wind speed (7-d moving average; dashed line) are shown in (f).

Variations in GPP_{SF} and GPP_{EC}

GPP values produced by the SF and EC estimations were in good agreement in 2010, with the regression producing a highly significant linear fit (Fig. 3; RMSE = 0.82). The 2005 comparison also produced similar GPP values for the two methods, with a linear regression slope of 1.045 ($r^2 = 0.64$, $P < 0.0001$). On the annual scale, GPP_{SF} underestimated the 2010 GPP_{EC} by 2.5%, with EC-derived GPP of 670 g C m^{-2} yr^{-1} compared with SF-derived GPP of 653 g C m^{-2} yr^{-1}. Note that in this overall good agreement some higher GPP_{SF}/GPP_{EC} ratios in some periods and lower ratios in others were neutralized (Table 2). Monthly GPP_{SF}/GPP_{EC} ratios were below or above 1.0 in wet season months (0.79 and 1.31 in January 2005 and January 2010) and in dry season months (0.55 and 1.37 in July and November 2010). Differences in GPP values between the methods mainly occurred at the onset of the growing season (mostly 21–29 January; Fig. 3c), at its end (mostly 7–14 April; Fig. 3d), and, to lesser extent, during July. GPP_{SF} overestimated the GPP_{EC} by up to 4.3 g C m^{-2} d^{-1} on 23 January, and underestimated the GPP_{EC} by up to 3.3 g C m^{-2} d^{-1} on 8 March. To test the inter-diurnal co-variability of GPP_{SF} and GPP_{EC}, a cross-correlation analysis was performed assuming time lags of 0–15 d (Fig. S3) producing the highest cross-correlation result at zero time lag ($r^2 = 0.82$). Figure 3(f) shows the GPP_{SF}/GPP_{EC} ratio, on a logarithmic scale, for 2010. The 10-fold GPP_{SF} overestimation on 28 January 2010 is evident, along with underestimations in October and December. The seasonal trend of good agreement between the methods in and after the wet season (February–June) and lesser agreement in the dry season (June–December) might indicate a limitation on the GPP_{SF} method at very low fluxes. The trends in the GPP_{SF}/GPP_{EC} dynamics (Table 2; Fig. 3f) hinted at possible contributions of environmental factors. The average wind speed showed some similarities to these dynamics (Fig. 3f). GPP_{SF}/GPP_{EC} was smaller than 1.0 in 73% of the days when wind speed < 2.5 m s^{-1}. Other environmental factors, such as VPD and soil moisture, were not related to GPP_{SF}/GPP_{EC} (Fig. S4). But generally both methods provided similar GPP estimates, as the GPP_{SF}/GPP_{EC} ratio was between 0.5 and 2.0 during 82% of the time.

Table 2 Monthly values of eddy covariance-derived and sap flow-derived gross primary productivity (GPP_{EC} and GPP_{SF}; g C m^{-2} per month) in Yatir forest in 2009–2010, and their ratios

Year	Month	GPP_{EC}	GPP_{SF}	GPP_{SF}/GPP_{EC} ratio
2005	**January**	122.1	96.5	0.79
	February	129.3	106.5	0.82
	March	193.2	N/A	N/A
	April	163.0	N/A	N/A
	May	101.2	N/A	N/A
	June	57.2	N/A	N/A
	July	33.0	31.6	0.96
	August	35.0	35.5	1.01
	September	31.4	24.2	0.77
	October	32.9	29.4	0.89
	November	40.1	31.0	0.77
	December	46.1	51.7	1.12
2009	October	14.6	12.8	0.88
	November	29.7	19.1	0.64
	December	31.1	19.6	0.63
2010	**January**	53.5	70.2	1.31
	February	95.2	99.8	1.05
	March	159.6	146.8	0.92
	April	117.8	148.8	1.26
	May	56.0	58.3	1.04
	June	31.0	23.5	0.76
	July	32.0	17.7	0.55
	August	24.7	17.8	0.72
	September	24.8	18.9	0.76
	October	20.4	18.7	0.92
	November	14.3	19.7	1.37
	December	17.5	19.9	1.14

Wet season months are given in boldface (May being wet in 2005 but not in 2010). GPP_{SF} values were not available (N/A) in March–June 2005 due to large data gaps.

Variations in GPP_{SF} and its components

The standard errors associated with variations among trees in SFD, interannual variations in WUE_i, and daytime fluctuations in VPD, were used in the calculation of the sources of variance in the GPP_{SF} estimation (Table 3). As expected, variations in GPP_{SF} were attributed mainly to variations in SFD, with VPD as the second source of variance, and smaller variance associated with WUE_i. The propagated error in GPP_{SF} estimation was relatively high, between 6.8% and 41.3% (Table 3). But notably, the higher relative errors were associated with the lower carbon fluxes in the dry season, and the absolute error was never above 1.0 g C m^{-2} d^{-1}. Overall, the mean relative error was 20.7%, which translates to 653 ± 135 g C m^{-2} yr^{-1} at the annual scale. The relationships between the SF-derived GPP, SFD and VPD_c were further tested (Fig. 4). As expected, GPP_{SF} correlated linearly with SFD, with some values along a maximum GPP_{SF} line and others distributed below this line (Fig. 4a). Most of these lower GPP_{SF} values were estimated for wet season days with increased VPD, potentially inducing partial stomatal closure and reduced assimilation. The association between GPP_{SF} and VPD_c was less strong (Fig. 4b), in line with the lesser role of VPD_c in determining GPP_{SF} (Table 3). Note that in our analysis VPD_c was constrained between 1.77 and 4.72 kPa, which are 1.18 of 1.5 and 4.0 kPa (see the Materials and Methods section). At any VPD_c there was large variance in GPP_{SF}, highlighting the role of additional drivers such as light, soil moisture and temperature. For example, $GPP_{SF} < 2.0$ g C m^{-2} d^{-1} was sometimes estimated on days with low VPD_c of 2.0 kPa. Such conditions prevailed during autumn, when VPD was decreasing but soil moisture was still too low to allow high assimilation rates. High rates of CO_2 uptake were usually related to mild VPD_c, and the maximum GPP_{SF} decreased by 1.64 g C m^{-2} d^{-1} for each 1.0 kPa increment in VPD_c.

Table 3 Error analysis for the sap flow-derived gross primary productivity (GPP) estimation method, with minimum and maximum standard errors (SE) associated with variations in sap flux density (SFD); interannual variations in the monthly mean intrinsic water-use efficiency (WUE_i), vapor pressure deficit (VPD), and the propagated standard error calculated for GPP

Parameter (unit)	SE range	Relative SE range (%)
SFD (cm^3 d^{-1} cm^{-2})	0.5–32.0	2.8–40.4
WUE_i (μmol CO_2 mol^{-1} H_2O)	0.3–7.0	0.3–7.9
VPD (kPa)	0.6–288.6	0.0–16.4
GPP (g C m^{-2} d^{-1})	0.0–1.0	6.8–41.3

Errors in the daily mean SFD were those associated with variations among the 10 individual trees; errors in the monthly mean WUE_i were from interannual variations in 2001–2003; and errors in the daily mean VPD were from fluctuations in the half-hourly VPD values during daytime.

Discussion

We presented the first comparison between SF-derived GPP and EC-derived GPP for a forest canopy. The GPP_{SF} captured the seasonal trends similarly to those measured by the GPP_{EC}, with GPP_{SF} values only slightly lower than GPP_{EC} values. This is noteworthy, especially considering that measurements are completely independent of each other: H_2O-based vs CO_2-based; and although in a uniform forest stand, the GPP_{SF} approach is tree-based near the flux tower and the EC-based one is atmospheric-based, capturing a fetch area away from the tower. The consistent agreement between the methods across seasons and years (Fig. 3a–e) provides some confidence in the robustness of the new GPP_{SF} approach. The annual GPP_{EC} and GPP_{SF} of 670 and 653 g C m^{-2} yr^{-1} translated into 22.3 and 21.8 kg C per tree yr^{-1}, reasonably close to the reported sum of tree C sinks of 23.5 kg C per tree yr^{-1} (Klein & Hoch, 2015). The high interdiurnal co-variability of GPP_{SF} and GPP_{EC} supports the idea that SF and $\delta^{13}C$-derived WUE can produce a mechanistically based proxy for GPP. Possible caveats are also indicated by the similar patterns of the GPP_{SF}/GPP_{EC} ratio and wind speed over part of the record. This may be related to increased EC measurement error at low wind speed (Nakai & Shimoyama, 2012) or increased transpiration (and hence GPP_{SF}) disproportional to CO_2 uptake at high wind speed. Variations in GPP_{SF} were mostly related to changes in SFD (Fig. 4; Table 3). Marked deviations were observed during the growth season onset, and in late April (Fig. 3f). These and other, smaller deviations

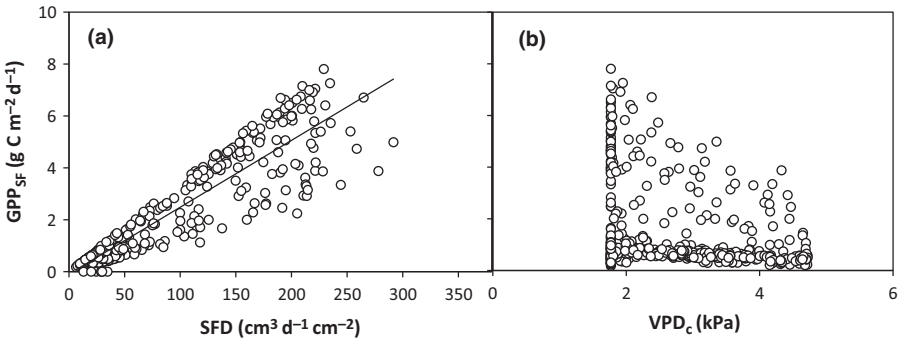

Fig. 4 Relationships between sap flow-derived gross primary productivity (GPP_{SF}) and sap flux density (SFD; a) and between GPP_{SF} and corrected vapor pressure deficit (VPD_c; b) in 2010. VPD_c was constrained between 1.77 and 4.72 kPa, which are 1.18 of 1.5 and 4.0 kPa, the lower and upper limits of CO_2 uptake sensitivity to VPD (see the Materials and Methods section) . The linear fit in (a) is: $GPP_{SF} = 0.027 \times SFD + 0.117$, $r^2 = 0.85$, $P < 0.0001$, $n = 457$ d.

occurred throughout the year and hence do not directly depend on seasonality (Table 2). In late January 2010 there was a 1-wk delay between the increase in GPP_{SF} on 21 January and the increase in GPP_{EC} on 28 January. If there was a decoupling between the trees' hydraulic and photosynthetic systems during the first week of the growing season, there should have been a transient decrease in WUE. It is possible that the December minimum in WUE_i (Fig. S2) is related to such scenario, but due to its short term, the transient low WUE_i values were potentially diluted by higher values during the same month. In mid-December 2001, a low WUE_i value of 70.5 μmol CO_2 mol^{-1} H_2O was calculated from chamber needle gas exchange measurements, immediately following a major rain event marking the onset of the growing season (Klein *et al.*, 2005). WUE_i values preceding and following this minimum by *c.* 1 month were 137.5 and 88.2 μmol CO_2 mol^{-1} H_2O, respectively. It is possible that following the dry season, the recovery of photochemistry and photosynthetic components in the needles (e.g. pigments, enzymes) was slower than that of the xylem, as shown elsewhere in olives and in oaks (Giorio *et al.*, 1999; Gallé *et al.*, 2007). Although these details need further studies and probably higher temporal resolution in the WUE estimates, it shows the potential in obtaining additional insights by constraining GPP using the two independent approaches.

It is difficult to relate our observations to those of earlier studies that measured GPP_{SF} but not GPP_{EC} (Hu *et al.*, 2010; Wang *et al.*, 2013). The forest settings of these earlier studies likely involved larger variations in the measured parameters than our semi-arid pine forest, for example related to a multiple number of tree species (Hu *et al.*, 2010). Nevertheless, both studies provided comparisons with other methodologies, and both reported consistently large underestimation of GPP by the SF-based method. The mean GPP_{SF} of a subalpine conifer forest (Hu *et al.*, 2010) was 0.97 g C m^{-2} d^{-1}, whereas the mean modeled GPP applied at the same site was 2.15 g C m^{-2} d^{-1}. In a subtropical acacia plantation (Wang *et al.*, 2013), the mean GPP_{SF} was 2.13 g C m^{-2} d^{-1}, whereas the mean GPP estimated from carbon balance for a similar ecosystem (Nouvellon *et al.*, 2012) was 8.77 g C m^{-2} d^{-1}. Here we estimated the mean GPP_{SF} and GPP_{EC} at 1.79 and 1.84 g C m^{-2} d^{-1}, respectively. A relatively good agreement between GPP_{EC} and GPP modeled using SF data (but not δ^{13}C-derived WUE_i) was also reported for a temperate pine species but not for deciduous species, possibly indicating higher complexity in GPP estimation in the latter (Schäfer *et al.*, 2003). Clearly this study benefitted from a combination of three SF measurement methods providing a robust T estimate verified by a closed water balance. For example, using noncalibrated readings from thermal dissipation SF probes would yield *c.* 60% lower SF values and GPP underestimation to match. Our calculation of WUE also improved on earlier studies (Hu *et al.*, 2010; Drake *et al.*, 2011), which didn't account for the advanced model of ^{13}C discrimination.

Uncertainties associated with the GPP_{SF} methodology

Our analysis highlighted the major contribution of the variations in SFD to the GPP_{SF} estimation (Table 3), also in agreement with the earlier applications of this methodology (Hu *et al.*, 2010; Wang *et al.*, 2013). At the single tree scale, SF integrates variations in transpiration rates across the tree crown, providing a rather robust T_{tree} flux for estimation of A_{tree}. However, at the canopy scale, differences among individual trees come into play, and can increase with competition for resources. The low water inputs in the semi-arid pine forest mean that even small structural changes in the soil and rhizosphere can translate into considerable differences in water uptake among neighboring trees. Evidence for such heterogeneity comes from a patchy spatial pattern of tree mortality observed in Yatir forest following the 2008–2009 drought (Klein *et al.*, 2014). Considering the observed variations in SFD (Fig. S1; Table 3), our analysis could benefit from a larger number of study trees.

The use of a single diurnal VPD value is a simplification that also increases the uncertainty of GPP_{SF}. Variations in VPD exist both in time (along the day and the year; Table 3) and space (across the canopy, from top to bottom, in shaded vs sunlit needles; Methods S2). Therefore, higher resolution data may produce more reliable estimates. Stomatal and photosynthetic effects were accounted for in our analysis, thereby limiting the VPD values to 1.5–4.0 kPa. We also calculated that the actual VPD at the leaf surface was *c.* 18% higher than the measured atmospheric VPD. Differences between air and needle temperatures, which were smaller than observed here, have been reported (Drake *et al.*, 2011), but increased with temperature. Note that the relationship between GPP_{SF} and VPD (Fig. 4a) is similar to the relationship between g_s and VPD reported earlier (Maseyk *et al.*, 2008), with the majority of values at low rates of g_s and GPP, associated with the long dry season, and a gradual decrease in the maximum values of g_s and GPP with increasing VPD.

The relatively small variations in $\delta^{13}C$-derived WUE_i meant a smaller effect on the GPP_{SF} error propagation than that of SFD and VPD (Table 3). Nevertheless, it is possible that concurrent, high-resolution wood sampling could improve our GPP estimations, as discussed above for the onset of the growth season. Concurrent sampling for $\delta^{13}C$ should also significantly reduce the number of samples by avoiding the need for a multi-annual average (Methods S1) but more work is needed to recommend a specific sampling density. Earlier studies provided alternative approaches in the sampling of organic matter for WUE_i estimation. The $\delta^{13}C$ signal of fresh leaf compounds might better represent the WUE_i of the photosynthates than the whole wood and needle samples used here, yet sugars are a relatively complex and dynamic pool and are not as integrative. The ratio WUE_i/VPD_c, which is equivalent to A_{tree}/T_{tree}, reproduced the A/T dynamics in these trees well, with wet season and dry season means of 4.5 and 3.1 mmol CO_2 mol^{-1} H_2O, respectively (Maseyk *et al.*, 2008).

At the forest scale, the GPP estimate is sensitive to variations in additional parameters, such as stand density and carbon uptake by understory vegetation. The latter parameter was estimated as very small in our study site (Grünzweig *et al.*, 2007), but water balance calculation showed that water use in the understory during the short wet season (and usually earlier than peak canopy activity) can be as high as 13% of the water budget (Klein *et al.*, 2014). Assuming that most of the understory gas exchange is indeed associated only with wet season growth of annuals and geophytes, its WUE should be lower than that of the pine trees, and hence the expected effect on GPP smaller than 13%. Nevertheless it must be recognized that relying on SF precludes consideration of the understory vegetation, which in some cases can be significant. When the contribution of the understory component is small, such as observed here, the GPP_{SF} and GPP_{EC} are expected to show high agreement and provide constraints and validation to either one of the approaches. Once faith in the robustness of the methodology is gained, the distinction between the two estimates should provide additional insights to ecosystem functioning.

Implications and perspectives

The encouraging outcome of our GPP_{SF} comparison study should motivate similar comparisons in other forest sites. Notably, such estimates can prove more complex than presented here due to higher ecosystem complexity. A major recommendation arising from this study is the requirement of intimate knowledge of the eco-physiology of the tree species in the studied canopy. For example, the response of g_s to VPD was critical for constraining high VPD values. The key role of GPP as a measure of the photosynthetic capacity of forests and its implications on the terrestrial carbon cycle, as conditions are changing, highlight the need to constrain and improve current GPP estimates. Although pronounced effort has been invested in setting up a global network of flux towers (www.fluxnet.ornl.gov), there is great need to increase the resolution of our observation across different vegetation types, land uses and climates. Recently, flux measurements of carbonyl sulfide (COS) have been utilized to infer ecosystem-scale GPP, and were in agreement with simultaneous GPP_{EC} within $\pm$ 15% (Asaf *et al.*, 2013). GPP_{COS} was usually higher than GPP_{EC}, especially in our semi-arid forest site. It seems that applying a combination of complementary approaches (e.g. GPP_{COS}, GPP_{SF} and GPP_{EC}) can produce a powerful measurement tool, both to constrain estimates of GPP and to provide additional insights based on the specific processes that control each methodology. Similarly, SF-measuring research stations, with and without flux towers, can become an important tool in he terrestrial carbon budgeting. The potential for enhancement and constraining of the global GPP monitoring network and database, and ultimately of global-scale GPP of the terrestrial biosphere, is hence considerable. Finally, the method presented here also offers a reasonable approach with which to reconstruct GPP using existing and archived datasets of SF and WUE, and to calculate additional parameters that are hard to obtain: for example, A_{tree}, the whole-tree C uptake and the mean stomatal conductance at the stand level.

Acknowledgements

The authors gratefully acknowledge Shabtai Cohen of ARO Volcani in Beit Dagan for providing sap flow data for 2005; Shmuel Spritzinn of the JNF-KKL for Yatir forest inventory data; and Rafael Poyatos of CREAF Barcelona and three anonymous referees for useful comments made on an earlier version of the paper. The KKL-JNF and the C. Wills and R. Lewis program in Environmental Science are greatly acknowledged for their financial support. T.K. is funded by Plant Fellows, an international Post doc Fellowship Program in Plant Sciences of the Zürich-Basel Plant Science Center (PSC). Research was co-funded by the EU FP7 Marie Curie actions (GA-2010-267243) and the Swiss National Science Foundation project FORCARB (31003A _14753/1).

References

Afik T. 2009. *Quantitative estimation of CO_2 fluxes in a semi-arid forest and their dependence on climatic factors.* MSc thesis submitted to R. H. Smith Faculty of Agriculture, Food and Environment of Hebrew University. Rehovot, Israel (in Hebrew).

Asaf D, Rotenberg E, Tatarinov F, Dicken U, Montzka SA, Yakir D. 2013. Ecosystem photosynthesis inferred from measurements of carbonyl sulphide flux. *Nature Geosciences* **6**: 186–190.

Aubinet M, Grelle A, Ibrom A, Rannik U, Moncrieff J. 2000. Estimates of the net carbon and water exchange of forests: the EUROFLUX methodology. In: Fitter A, Raffaeli D, eds. *Advances in ecological research 30.* Massachusetts, MA, USA: Academic Press, 113–175.

Baldocchi DD. 2003. Assessing the eddy covariance technique for evaluating carbon dioxide exchange rates of ecosystems: past, present and future. *Global Change Biology* **9**: 479–492.

Baldocchi D, Falge E, Gu L, Olson R, Hollinger D, Running S, Anthoni P, Bernhofer C, Davis K, Evans R *et al.* 2001. FLUXNET: a new tool to study the temporal and spatial variability of ecosystem-scale carbon dioxide, water vapor, and energy flux densities. *Bulletin of the American Meteorological Society* **82**: 2415–2434.

Bar Massada A, Carmel Y, Tzur GE, Grünzweig JM, Yakir D. 2006. Assessment of temporal changes in aboveground forest tree biomass using aerial

photographs and allometric equations. *Canadian Journal of Forest Research* **36**: 2585–2594.

Beer C, Ciais P, Reichstein M, Baldocchi D, Law BE, Papale D, Soussana J-F, Amman C, Buchmann N, Frank D *et al.* 2009. Temporal and among-site variability of inherent water use efficiency at the ecosystem level. *Global Biogeochemical Cycles* **23**: GB2018.

Beer C, Reichstein M, Tomelleri E, Ciais P, Jung M, Carvalhais N, Rödenbeck C, Altaf Arain M, Baldocchi D, Bonan GB *et al.* 2010. Terrestrial gross carbon dioxide uptake: global distribution and covariation with climate. *Science* **329**: 834–838.

Bonan GB. 2008. Forests and climate change: forcings, feedbacks, and the climate benefits of forests. *Science* **320**: 1444–1449.

Canadell JG, Raupach MR. 2008. Managing forests for climate change mitigation. *Science* **320**: 1456–1457.

Cermak J, Kucera J, Nadezhdina N. 2004. Sap flow measurements with some thermodynamic methods, flow integration within trees and scaling up from sample trees to entire forest stands. *Trees* **18**: 529–546.

Ciais P, Reichstein M, Viovy N, Granier A, Ogee J, Allard V, Aubinet M, Buchmann N, Bernhofer C, Carrara A *et al.* 2005. Europe-wide reduction in primary productivity caused by the heat and drought in 2003. *Nature* **437**: 529–533.

Cohen Y, Cohen S, Cantuarias-Aviles T, Schiller G. 2008. Variations in the radial gradient of sap velocity in trunks of forest and fruit trees. *Plant and Soil* **305**: 49–59.

Drake JE, Davis SC, Raetz LM, DeLucia EH. 2011. Mechanisms of age-related changes in forest production: the influence of physiological and successional changes. *Global Change Biology* **17**: 1522–1535.

Ewers BE, Oren R. 2000. Analyses of assumptions and errors in the calculation of stomatal conductance from sap flux measurements. *Tree Physiology* **20**: 579–589.

Farquhar GD, Richards RA. 1984. Isotopic composition of plant carbon correlates with water-use efficiency of wheat genotypes. *Functional Plant Biology* **11**: 539–552.

Gallé A, Haldimann P, Feller U. 2007. Photosynthetic performance and water relations in young pubescent oak (*Quercus pubescens*) trees during drought stress and recovery. *New Phytologist* **174**: 799–810.

Giorio P, Sorrentino G, d'Andria R. 1999. Stomatal behaviour, leaf water status and photosynthetic response in field-grown olive trees under water deficit. *Environmental & Experimental Botany* **42**: 95–104.

Granier A. 1985. A new method of sap flow measurement in tree stems. *Annals of Forest Science* **42**: 193–200.

Grünzweig JM, Gelfand I, Yakir D. 2007. Biogeochemical factors contributing to enhanced carbon storage following afforestation of a semi-arid shrubland. *Biogeosciences* **4**: 891–904.

Grünzweig JM, Lin T, Rotenberg E, Schwartz A, Yakir D. 2003. Carbon sequestration in arid-land forest. *Global Change Biology* **9**: 791–799.

Grünzweig JM, Hemming D, Maseyk K, Lin T, Rotenberg E, Raz-Yaseef N, Falloon PD, Yakir D. 2009. Water limitation to soil CO_2 efflux in a pine forest at the semiarid "timberline". *Journal of Geophysical Research: Biogeosciences* **114**: doi: 10.1029/2008JG000874.

Heskel MA, Bitterman D, Atkin OK, Turnbull MH, Griffin KL. 2014. Seasonality of foliar respiration in two dominant plant species from the Arctic tundra: response to long-term warming and short-term temperature variability. *Functional Plant Biology* **41**: 287–300.

Hu J, Moore DJ, Riveros-Iregui DA, Burns SP, Monson RK. 2010. Modeling whole-tree carbon assimilation rate using observed transpiration rates and needle sugar carbon isotope ratios. *New Phytologist* **185**: 1000–1015.

Kanety T. 2010. Yield and physiological and environmental water stress indicators of persimmon trees irrigated with different amounts of recycled water. MSc thesis, The Hebrew University of Jerusalem, Rehovot, Israel.

Klein T, Hemming D, Lin T, Grünzweig JM, Maseyk KS, Rotenberg E, Yakir D. 2005. Association between tree-ring and needle delta ^{13}C and leaf gas exchange in *Pinus halepensis* under semi-arid conditions. *Oecologia* **144**: 45–54.

Klein T, Hoch G. 2015. Tree carbon allocation dynamics determined using a carbon mass balance approach. *New Phytologist* **205**: 147–159.

Klein T, Rotenberg E, Cohen-Hilaleh E, Raz-Yaseef N, Tatarinov F, Preisler Y, Ogee J, Cohen S, Yakir D. 2014. Quantifying transpirable soil water and its relations to tree water use dynamics in a water-limited pine forest. *Ecohydrology* **7**: 409–419.

Luyssaert S, Inglima I, Jung M, Richardson AD, Reichstein M, Papale D, Piao SL, Shulze E-D, Wingate L, Matteucci G *et al.* 2007. CO_2 balance of boreal, temperate, and tropical forests derived from a global database. *Global Change Biology* **13**: 2509–2537.

Maseyk K, Grünzweig JM, Rotenberg E, Yakir D. 2008. Respiration acclimation contributes to high carbon-use efficiency in a seasonally dry pine forest. *Global Change Biology* **14**: 1–15.

Maseyk K, Hemming D, Angert A, Leavitt SW, Yakir D. 2011. Increase in water-use efficiency and underlying processes in pine forests across a precipitation gradient in the dry Mediterranean region over the past 30 years. *Oecologia* **167**: 573–585.

Nakai T, Shimoyama K. 2012. Ultrasonic anemometer angle of attack errors under turbulent conditions. *Agricultural and Forest Meteorology* **162**: 14–26.

Nouvellon Y, Laclau JP, Epron D, Le Maire G, Bonnefond JM, Gonçalves JLM, Bouillet JP. 2012. Production and carbon allocation in monocultures and mixed-species plantations of *Eucalyptus grandis* and *Acacia mangium* in Brazil. *Tree Physiology* **32**: 680–695.

Parazoo NC, Bowman K, Fisher JB, Frankenberg C, Jones DBA, Cescatti A, Perez-Priego O, Wohlfahrt G, Montagnani L. 2014. Terrestrial gross primary production inferred from satellite fluorescence and vegetation models. *Global Change Biology* **20**: 3103–3121.

Paudel I, Kanety T, Wachsmann Y, Sadka A, Cohen S. 2013. Inactive xylem can explain differences in calibration factors for thermal dissipation probe sap flow measurements. *Tree Physiology* **33**: 986–1001.

Raz-Yaseef N, Yakir D, Rotenberg E, Schiller G, Cohen S. 2010. Ecohydrology of a semi-arid forest: partitioning among water balance components and its implications for predicted precipitation changes. *Ecohydrology* **3**: 143–154.

Reichstein M, Bahn M, Ciais P, Frank D, Mahecha MD, Senevirante SI, Zcheiscler J, Beer C, Buchmann N, Frank DC *et al.* 2013. Climate extremes and the carbon cycle. *Nature* **500**: 287–295.

Reichstein M, Falge E, Baldocchi D, Papale D, Aubinet M, Berbigier P, Bernhofer C, Buchmann N, Gilmanov T, Granier A *et al.* 2005. On the separation of net ecosystem exchange into assimilation and ecosystem respiration: review and improved algorithm. *Global Change Biology* **11**: 1424–1439.

Rotenberg E, Yakir D. 2010. Contribution of semi-arid forests to the climate system. *Science* **327**: 451–454.

Schäfer KV, Oren R, Ellsworth DS, Lai C-T, Herrick JD, Finzi AC, Richter DD, Katul GG. 2003. Exposure to an enriched CO_2 atmosphere alters carbon assimilation and allocation in a pine forest ecosystem. *Global Change Biology* **9**: 1378–1400.

Seibt U, Rajabi A, Griffiths H, Berry JA. 2008. Carbon isotopes and water use efficiency: sense and sensitivity. *Oecologia* **155**: 441–454.

Speckman HN, Frank JM, Bradford JB, Miles BL, Massman WJ, Parton WJ, Ryan MG. 2014. Forest ecosystem respiration estimated from eddy covariance and chamber measurements under high turbulence and substantial tree mortality from bark beetles. *Global Change Biology* **21**: 708–721.

Steppe K, De Pauw DJW, Doody TM, Teskey ROA. 2010. Comparison of sap flux density using thermal dissipation, heat pulse velocity and heat field deformation methods. *Agricultural & Forest Meteorology* **150**: 1046–1056.

Tatarinov FA, Kučera J, Cienciala E. 2005. The analysis of physical background of tree sap flow measurement based on thermal methods. *Measurement Science & Technology* **16**: 1157.

Taylor JR. 1997. *An introduction to error analysis.* Sausalito, CA, USA: University Science Books.

Van Gorsel E, Delpierre N, Leuning R, Black A, Munger JW, Wofsy S, Aubinet M, Feigenwinter C, Berniger J, Bonal D *et al.* 2009. Estimating nocturnal ecosystem respiration from the vertical turbulent flux and change in storage of CO_2. *Agricultural and Forest Meteorology* **149**: 1919–1930.

Von Caemmerer SV, Farquhar GD. 1981. Some relationships between the biochemistry of photosynthesis and the gas exchange of leaves. *Planta* **153**: 376–387.

Wang H, Zhao P, Zou LL, McCarthy HR, Zeng XP, Ni GY, Rao XQ. 2013. CO_2 uptake of a mature *Acacia mangium* plantation estimated from sap flow measurements and stable carbon isotope discrimination. *Biogeosciences Discussions* **10**:11583–11625.

Supporting Information

Additional supporting information may be found in the online version of this article.

Fig. S1 Variations in sap flow and sap flux density as a function of tree diameter at breast height among the 10 measured *Pinus halepensis* trees in Yatir forest.

Fig. S2 Changes in intrinsic water-use efficiency of *Pinus halepensis* in Yatir forest, from chamber measurements of assimilation and stomatal conductance and from $\delta^{13}C$ of needles and stem wood.

Fig. S3 Cross-correlation analysis between GPP_{SF} and GPP_{EC} and between $dlnGPP_{SF}$ and $dlnGPP_{EC}$, where $dlnGPP = (GPP_{day\ i-1} - GPP_{day\ i})/GPP_{day\ i-1}$.

Fig. S4 Relationships between the GPP_{SF}/GPP_{EC} ratio and the prevailing vapor pressure deficit and soil water content.

Methods S1 Estimation of WUE_i from wood and needle $\delta^{13}C$.

Methods S2 Validations of the vapor pressure deficit (VPD) measurement.

Please note: Wiley Blackwell are not responsible for the content or functionality of any supporting information supplied by the authors. Any queries (other than missing material) should be directed to the *New Phytologist* Central Office.